Bulletin of the JSME Vol.9, No.2, 2014
Journal of Thermal Science and Technology

Investigation of fuel reduction effect of the Antarctic Syowa Base microgrid by introduction of local-supply-and-local-consumption energy

Shin'ya OBARA*, Takuya KANAI*, Kenji ISHIZAWA** and Jorge Morel*
* Department of Electrical and Electronic Engineering, Kitami Institute of Technology
165, Koen-cho, Kitami, Hokkaido 090-8507, Japan
E-mail: obara@mail.kitami-it.ac.jp
**National Institute of Polar Research Japan
10-3, Midori-cho, Tachikawa-shi, Tokyo 190-8518, Japan

Received 20 August 2014

Abstract
A small-scale energy network present at the Antarctic Syowa Base (Syowa Base microgrid, SBMG) has issues related to the amount of fuel transported from Japan and the environmental impact from emissions. Therefore, the Syowa Base is considering the introduction of photovoltaics (PV) and wind power generations to drastically increase the local supply and consumption of energy. After the introduction of a type of heat supply system, heat pump system, using engine exhaust heat and an electric storage heater hybrid system into SBMG, the reduced introductory rate of renewable energy and fuel consumption at the Syowa Base was investigated. Results confirmed a reduction in fuel consumption of the base by heat storage using renewable energy, following the introduction of a heat pump and electric storage heater hybrid system. However, for the electric storage heater to function year round, extensive wind power generation was required. The heat pump and electric storage heater hybrid system reduced fuel consumption of the Syowa Base by 15 % in January. On the other hand, hybrid systems reduced fuel consumption to about half of the present system. Fuel reduction was not observed in July and October because these months had a much greater heat demand. Reduction in fuel consumption of the whole base required an increase in the amount of wind power generation, which was influenced very little by the seasonal changes, and an optimization of the electric storage heater operation.

Key words : South Pole, Microgrid, Syowa base, Heat pump, Electric storage heater

1. Introduction

The Antarctic Syowa Base was established as an observation post for the Japanese Antarctic area in the east Ongul (69° 00′ S, 39° 35′ E, altitude of 29 m) in 1957. The National Institute of Polar Research of Japan has jurisdiction over the Syowa Base and the following base camps: Mizuho base, Asuka base and Dome Fuji observation base. At present, the Syowa Base consists of 70 buildings, and the energy is predominantly supplied by fossil fuels and minimally by renewable energy (photovoltaics (PV) and wind power generation). However, with the construction of the green-energy research building, which began with the arrival of the 51st party (February, 2010–January, 2011), henceforth, it is necessary to consider the construction of a small-scale energy network (Syowa Base microgrid: SBMG) to enable local supply and consumption of energy. Although the introduction of photovoltaics and wind power generation has been tried at the Syowa Base, at present the main power supply is a 240 kW diesel engine generator (centralization power supply system). An increase in the local supply and consumption of energy is drastically needed for the reduction of fuel transport from Japan and to minimize the environmental impact of emissions (Nishikawa, et al., 2011, National Institute of Polar Research Japan, 2011). Therefore, in this study, distribution methods of a small capacity engine generator (distributed power supply system) were investigated. Furthermore, to maintain a high COP (coefficient of performance), the introduction of a heat pump system using engine exhaust heat was investigated as a heat source (Obara,

Paper No.14-00347
[DOI: 10.1299/jtst.2014jtst0013]

et al., 2013). Many studies have investigated the efficient arrangement and distribution of engine generators (Dawei, et al., 2013, Uisung, 2013, Massimiliano, 2011). Previous studies have clarified the role of the distribution of engine generators, the heat pump system using engine exhaust heat, relationship between the amount of photovoltaics and wind power generation introduced, and fuel consumption needs of the base (Obara, et al., 2013). If the amount of renewable energy to SBMG increases, a large period shift of electricity and heat will be required to balance supply and demand. The use of a battery for electricity storage has been previously reported (Obara, et al., 2013), detailing the use of a heat storage tank and optimizing the storage capacity. Since the heat pump system using engine exhaust heat can maintain high COP, the introduction of the heat pump system can vastly cut down fuel consumption requirements by the heat load of SBMG. However, because it is necessary to install the heat pump systems using engine exhaust heat near the engines, the placement of heat pumps is restricted. Moreover, it is difficult for 70 buildings to distribute heat using a heat pump. Therefore, installation of electric storage heaters (Homepage of Telegraph Media Group Limited, 2014), which are currently widely used by super airtight and super insulation houses of cold district, and storage of the electricity by renewable energy in each SBMG building is required. The heating capacity of an electric storage heater is decided by its heating storage capacity and heat radiating ability (there is a type of free convection or forced convection). Although the electric storage heater is economically disadvantageous to the heat pump accompanied by COP of 1.0 or more, clean and safe space heating is enabled by the installation of a power line. Heat storage technology using renewable energy has often been investigated, and it can account for output fluctuations of green energy (Arteconi, et al., 2012, Chesi, et al., 2013, Tian and Zhao, 2013).

When the introduction of renewable energy to SBMG is greatly increased, periods of surplus power will increase. The surplus power must be stored as electricity or stored heat. In this study, we look at installing electric storage heaters in each building and storing surplus power through a power grid of SBMG. On the other hand, heat pump systems are also introduced in buildings with large heat demands, such as residence building, and electric storage heaters are introduced in other buildings. The purpose of this study is to investigate reduction in fuel consumption of the base following the introduction of the hybrid heat feeding system of heat pumps using engine exhaust heat and electric storage heaters into SBMG, when the rate of renewable energy is increased. The introduction of electric storage heaters can be done implemented by two methods: (1) without control of a power supply; and (2) with an operation planning and control of a power supply. The former method (1) is used in this study. Therefore, electric storage heaters are added to the analytic model of a previous study (Obara, et al., 2013), and the relationship between the amount of introduction and fuel consumption of renewable energy in the Syowa Base is investigated. The effect of electric storage heaters is recognized in this study by the planning and controlling of the power supply to electric storage heaters (2) described above. The operation method for the maximum reduction of fuel consumption is clarified in the following section.

2. Scheme and energy balance of Syowa Base microgrid

2.1 Present Fuel Consumption in the Syowa Base

Figure 1 shows the arrangement of buildings at the Antarctic Syowa Base in 2011, and a scheme of electric power and heat equipment. However, photovoltaics and wind power generation are referred to as renewable energy in Fig. 1, and are soon to be introduced in large quantities. There are installations other than 70 buildings (gross floor area of 6981 m^2), such as water storage tanks, various antennas, and storage oil tanks, at the Syowa Base. The accommodation space centering on the administration building (A_4 in Fig. 1) of the base was serviced from 1991, and the base consists of three power-generation buildings (A_0, B_0, H_2), two residence buildings (A_1, A_2), 19 observation and research buildings, four warehouses, one car barn, and various other buildings. The heat for space heating and hot-water supply of the Syowa Base is presently provided by exhaust heat of an engine generator, electric heaters, kerosene boilers, oilstoves, and a solar collector. Moreover, main power supply at present is a diesel engine generator of 240 kW. It is installed in the power-generation building (A_0). Exhaust heat of the engine installed in A_0 is currently heating the power-generation, storage and sewage disposal (A_3), administration (A_4), and residence (A_1, A_2) buildings. Electric heaters, kerosene boilers, oilstoves, and a solar collector are used for space heating and hot-water supply of other buildings. 430 kL of fuel for power generation and 87 kL of fuel for space heating are currently consumed every year at the Syowa Base (a reserve is included) (Nishikawa, et al., 2011, National Institute of Polar Research Japan, 2011). In this study, the present SBMG described above is defined as the conventional system. The aim of this study is to drastically reduce fuel consumption for power generation and space heating of the conventional system. The fuel of the Syowa Base is transported once a year from Japan by the observatory ship Shirase. The diesel fuel of 430 kL described above includes

[DOI: 10.1299/jtst.2014jtst0013]

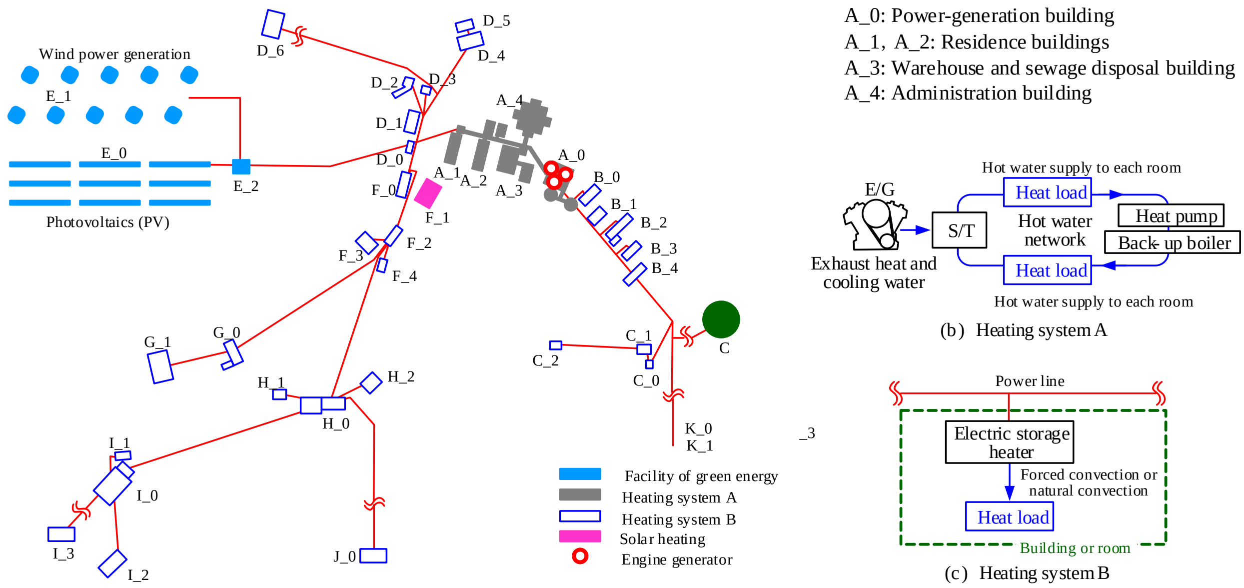

Fig. 1 Configuration of the electric power network and heating system of the Syowa Base

the heat demand of space heating of a residence building, an administration building, power-generation buildings, a storage building, and sewage disposal buildings (A_0–A_4), hot-water supply, and a thaw (life water) other than the power supply of the whole Syowa Base. Furthermore, in addition to the consumption of 90 kL of engine oil, the space heating of buildings other than those described above is provided by 87 kL of JP-5 fuel yearly.

2.2 Proposed SBMG

To increase the introductory rate of SBMG green energy, the present concentration power currently installed in the power-generation building (A_0) was distributed and arranged to three sets of small capacity. The distributed power supply described above is interconnected through SBMG with photovoltaics (E_0) and wind power generation (E_1). On the ridge near engine generators, for the power-generation, storage and sewage disposal, administration, and residence buildings, heat is provided with heat pumps using engine exhaust heat, heat storage tanks, and backup boilers. The supply capability for SBMG is two or more sets of diesel engine generators, photovoltaics (E_0), and wind power generation (E_1) described above. Electricity is provided to a power network by interconnecting each supply capability. Moreover, electric storage heaters are installed in each ridge, except for the buildings described above and the green energy building (F_1). Space heating at the base by electric storage heaters is easy and safe. The introduction of electric storage heaters will stabilize green energy fluctuations. Moreover, from the control room installed in the administration building, space heating of all ridges is easily manageable. The heat for space heating, hot-water supply, and a thaw (life water) for the residence, and administration, power-generation, storage, and sewage disposal (from A_0 to A_4) buildings is provided by heat pumps using exhaust heat of engine generators and backup boilers proposed for SBMG. Other buildings are heated by electric storage heaters and the conventional solar collector.

2.3 Energy Balance

2.3.1 Energy Flow of Proposed System

Figure 2 shows the energy flow of the proposed system. A set of three small-scale engine generators, a wind power generation, and photovoltaics are installed for the supply side of the power network. The common power load of the whole base, heat pumps, and electric storage heaters are represented as the demand side. Furthermore, as described in Section 3.1, the minimum accumulation-of-electricity system, for avoiding partial load operations of engine generators, was installed. The low temperature heat source of the heat pump is the engine exhaust heat after supplying heat to a part of demand side. Actually, the heat medium (antifreezing solution) that was heat-exchanged with engine exhaust heat in an exhaust heat exchanger was supplied to the demand side. If engine exhaust heat is used as a heat source for the heat pump, a high COP is expected for the pump because the temperature of the heat source is higher than the open air. However, since the capacity of the heat pump is restricted to the engine exhaust heat, the installation of backup boilers (B0, B1, and B2) after the heat pump, as shown in Fig. 2, is assumed as per the analytic model. Accordingly, when the

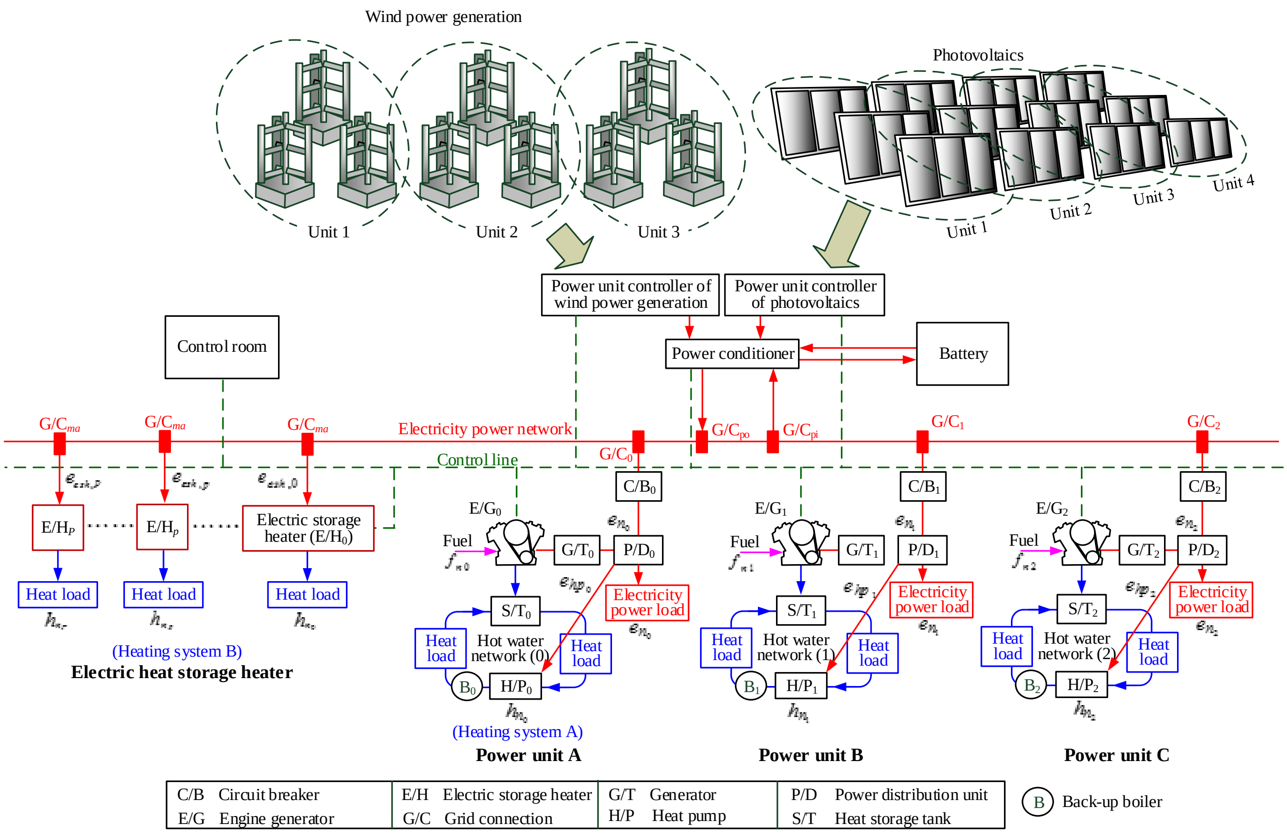

Fig. 2 Energy flow of the proposed microgrid

heat source of heat pumps is less than the engine exhaust heat, the backup boiler is operated.

2.3.2 Electric Power

Equation (1) is the balance formula of electricity in sampling time t of SBMG, as shown in Fig. 2. The left-hand side of Eq. (1) represents power items of electricity, and the right-hand side the consumption items of electricity. N_{pvu} is a set of photovoltaics with a power of e_{pv}, N_{wpu} is a set of wind turbines with a power generation of e_{wp}, and N_{eg} is a set of engine generators with a power of e_{eg} and input and output of a storage battery of e_{bt}. On the other hand, electricity is consumed by electricity demand Δe_{load} on the right-hand side of Eq. (1), where, N_{eg} is a set of heat pumps with a of power consumption of Δe_{hp}, N_{esh} a set of electric storage heaters with a power consumption of Δe_{esh}, and loss of is Δe_{loss}. Loss of a power conditioner of photovoltaics, a storage battery, and loss of generators are included in Δe_{loss}.

$$\sum_{i=1}^{N_{pvu}} e_{pv,i} + \sum_{j=1}^{N_{wpu}} e_{wp,j} + \sum_{k=1}^{N_{eg}} e_{eg,k} + e_{bt} = \Delta e_{load} + \sum_{m=1}^{N_{eg}} \Delta e_{hp,m} + \sum_{n=1}^{N_{esh}} \Delta e_{esh,n} + \Delta e_{loss} \quad (1)$$

2.3.3 Heat

Equation (2) is the heat balance equation for a sampling time t in SBMG. The left hand side of Eq. (2) represents the output in terms of heat, and the right hand side represents the output in terms of heat load. Heat is supplied to a N_{loadh} set of heat load Δh_{load} from a N_{eg} set of the thermal power h_{eg} of the engine generators, a N_{esh} set of the thermal power h_{esh} of electric storage heaters, a N_{eg} set of the thermal power h_{hp} and h_{bo} of heat pumps and the backup boilers, and a N_{eg} set of the thermal power h_{hst} of the input and output of the heat storage tanks. Moreover, Δh_{loss} refers to heat loss, radiation loss and thermal-storage loss of all equipment.

[DOI: 10.1299/jtst.2014jtst0013]

$$\sum_{k=1}^{N_{eg}} h_{eg,k} + \sum_{n=1}^{N_{esh}} h_{esh,n} + \sum_{m=1}^{N_{eg}} h_{hp,m} + \sum_{o=1}^{N_{eg}} h_{bo,o} + \sum_{k=1}^{N_{eg}} h_{hst,k} = \sum_{p=1}^{N_{loadh}} \Delta h_{load,p} + \Delta h_{loss} \tag{2}$$

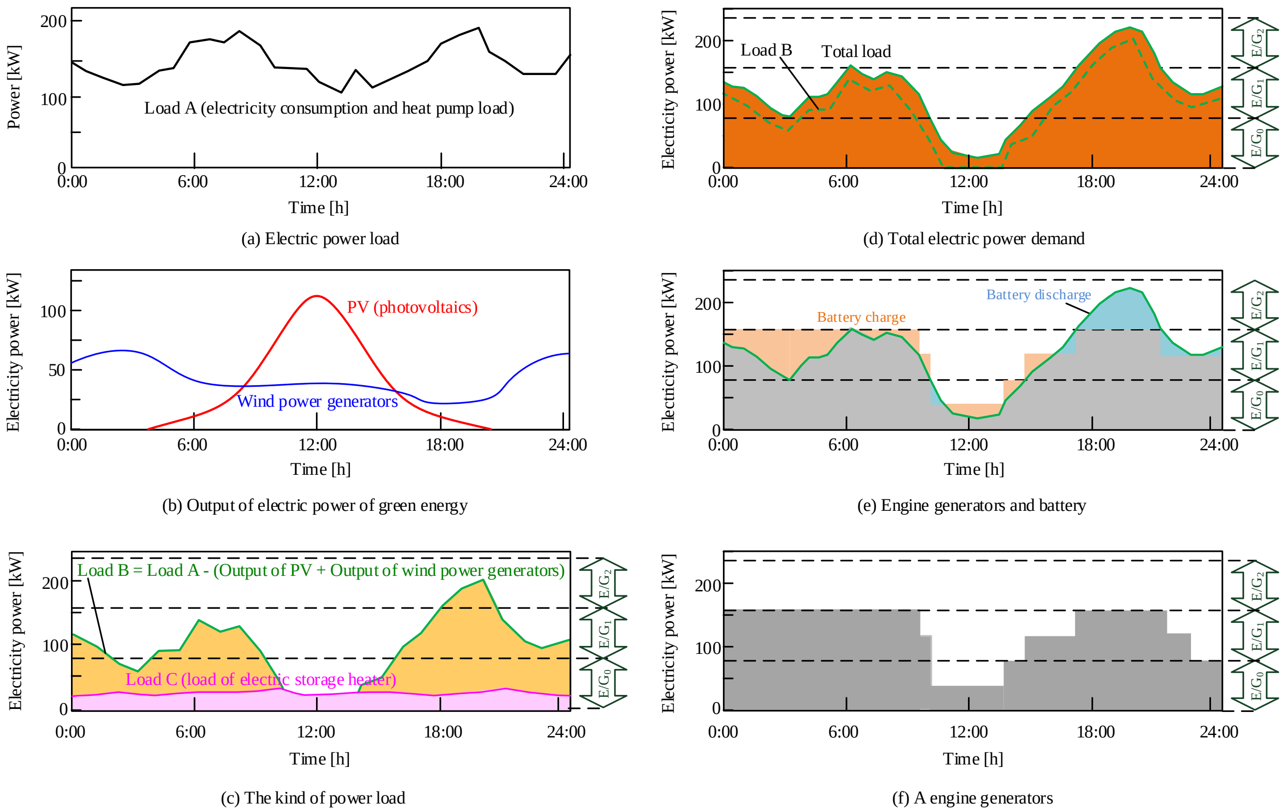

Fig. 3 Proposed operation planning of the SBMG

3. Operation Method of the System

3.1 Power Supply System

Figure 3 shows the operation method of the distributed engine generators installed in SBMG. Figure 3 (a) is an example of a power load pattern at the Syowa Base on a representative day, and the power load is described as Load A. The common power load of the base and the power load of heat pumps are included in Load A. Figure 3 (b) shows a power pattern of renewable energy (photovoltaics and wind power generator). In this case, Load B in Fig. 3 (c) is the load minus the production of electricity by renewable energy from Load A; Load C in the figure is the load of electric storage heaters. The sum total of Load B and Load C in Fig. 3 (c) is Total load in Fig. 3 (d). In the proposed system, the Total load in Fig. 3 (d) is supplied with three sets of small-scale engine generators.

Although the operation of three sets of engine generators (E/G$_0$, E/G$_1$, E/G$_2$) is controlled according to the magnitude of the Total load, when fluctuation in the load occurs with periods of low power generation efficiency, a partial load operation of the engine generators will occur. Moreover, when the load is small, maintenance of stable operation generally becomes difficult. Therefore, the minimum load factor of all engine generators of the distributed power supply system is set to 50%, and the engine generators are operated at 0% (neutral operation), 50%, or 100% of each rated power. When the power of the engine generators is set to 0%, 50%, or 100%, the supply and demand electricity balance occurs for periods of surplus and shortage, as shown in Fig. 3 (e). Therefore, the supply and demand electricity balance is adjusted by charge and discharge of the storage battery, as shown in Fig. 3 (e). As a result, each engine generator can obtain a high power load factor across various time periods, as shown in Fig. 3 (f). Furthermore, because there are no hours of operation for E/G$_2$, one-set engine generators are reducible, as shown in Fig. 3 (f).

Electricity to electric storage heaters is supplied from an electric power system accompanied by renewable energy and engine generators. Therefore, in periods of minimal electricity production from renewable energy, electricity is automatically supplied to electric storage heaters from engine generators. Moreover, as the broken green line in Fig. 2 shows, starting, stopping, output adjustment of each engine generator, measurement of frequency and voltage of a the power network, power supply to electric storage heaters, output adjustment of heat pumps, measurement of the circulation

[DOI: 10.1299/jtst.2014jtst0013]

hot water temperature for space heating (heat medium), power measurement of green energy, and the activity of wind power generation are all controlled by the control console.

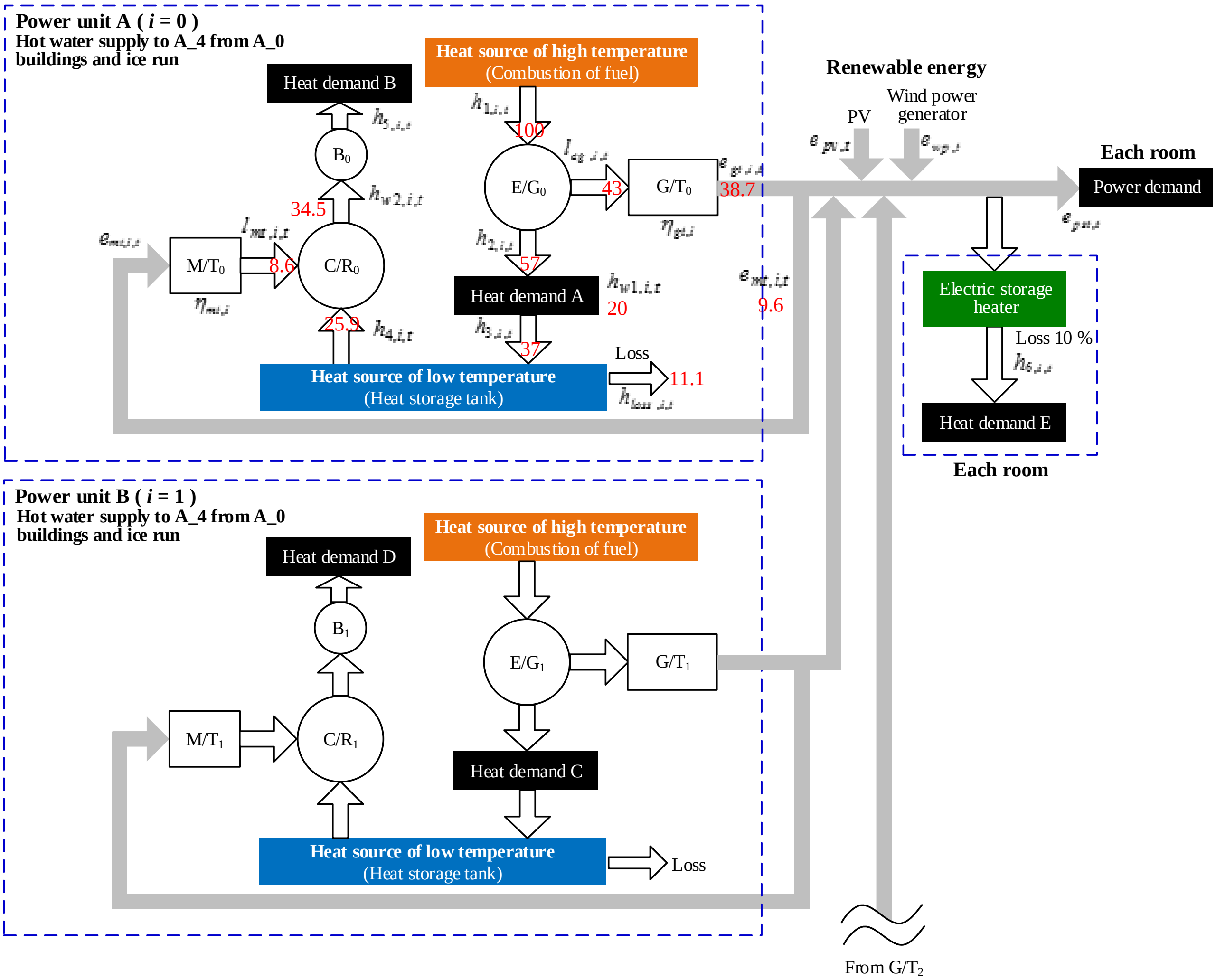

Fig. 4 Energy flow

3.2 Heat Supply System

Figure 4 is a configuration figure of heat engines and heat pumps introduced into the proposed SBMG, where the calorific value of fuel $h_{1,i,t}$ outputs the external work $l_{eg,i,t}$ and the exhaust heat $h_{2,i,t}$. When $l_{eg,i,t}$ is given to the power generator (G/T$_i$) controlling the power-generation efficiency $\eta_{gt,i}$, the electricity $e_{gt,i,t}$ will be outputted in the power network. The electricity of photovoltaics $e_{pv,t}$ and the electricity of wind power generation $e_{wp,t}$, other than $e_{gt,i,t}$, are supplied to the power network. At the same time, electricity is consumed with the power load in the base $e_{pst,t}$ and the power load of the heat pump $e_{mt,i,t}$. The red numbers in the Power unit A of Fig. 4 are energy distribution based on the fuel calorific value ($h_{1,i,t}$) of the engine generator at the time of rated operation, where, efficiency of the generator $\eta_{gt,i}$, efficiency of electric motor of the heat pump $\eta_{mt,i}$, and COP were set to 0.9, 0.9, and 4.0, respectively. Furthermore, the sum total of mechanical loss of the engine generator and radiation losses, such as from the engine, the heat storage tank, and piping, was determined and set from past records at about 11 % of the fuel calorific value. Heat demand is divided into Heat demand A and Heat demand B (case of i = 0) in the figure. A part of the engine exhaust heat $h_{2,i,t}$ is supplied to Heat demand A, and the sum total of heat $h_{5,i,t}$ from the heat pump $h_{w2,i,t}$ and the heat from the backup boiler $h_{5,i,t}$, is supplied to Heat demand B. When not taking into consideration the power supply by green energy, the maximum output of the heat pump is 34.5% of the fuel heating value $h_{1,i,t}$. Power of the heat pump $h_{w2,i,t}$ is the sum of the heating value $h_{4,i,t}$ of the heat source at low temperatures and the power $l_{mt,i,t}$ of the electric motor. Therefore, even if a large amount of electricity is supplied by green energy to the heat pump, the power of the heat pump $h_{w2,i,t}$ is restricted to the magnitude of $h_{4,i,t}$. The electric storage heater uses the engine generator and interconnection

[DOI: 10.1299/jtst.2014jtst0013]

electric power of renewable energy, as shown in Fig. 4. Although various methods relating to the operation of electric storage heaters were assumed, electric storage heaters are always connected to the power grid, and the loss is determined at 10% of electricity inputs.

4. Equipment characteristics
4.1 Engine generator

Three sets of 113 kW engine generators (i = 0, 1, or 2) were introduced as the main power supply of SBMG. Engine generators are the widely used products in Japan, and the power generation efficiency $\eta_{ege,i}$ is shown in Eq. (3), which is based on the engine load factor $\lambda_{eg,i}$ and the efficiency of the generator $\eta_{gt,i}$ (Uisung, et al., 2013). Although the maximum engine efficiency is 43.6%, the loss of the power generator is 10%, and the maximum power generation efficiency is 39.2%. Since the actual radiation loss or engine performance for the heat exchanger is unknown, calculation of the amount of exhaust heat of the engine generator refers to the overall efficiency of the 240 kW concentration type engine power generators.

$$\eta_{ege,i} = \left(-0.00000356 \cdot \lambda_{eg,i}^2 + 0.001493 \cdot \lambda_{eg,i} + 0.3128\right) \cdot \eta_{gt,i} \tag{3}$$

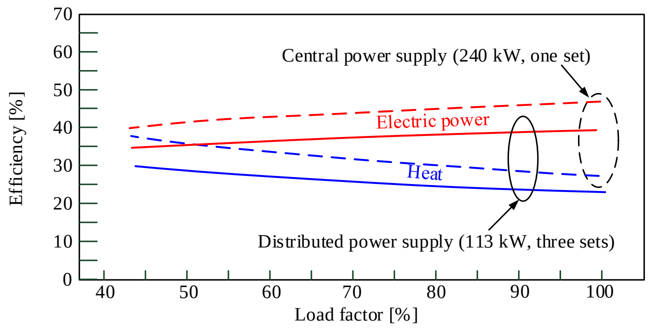

Fig. 5 Performance of the engine generator of a central and distributed system

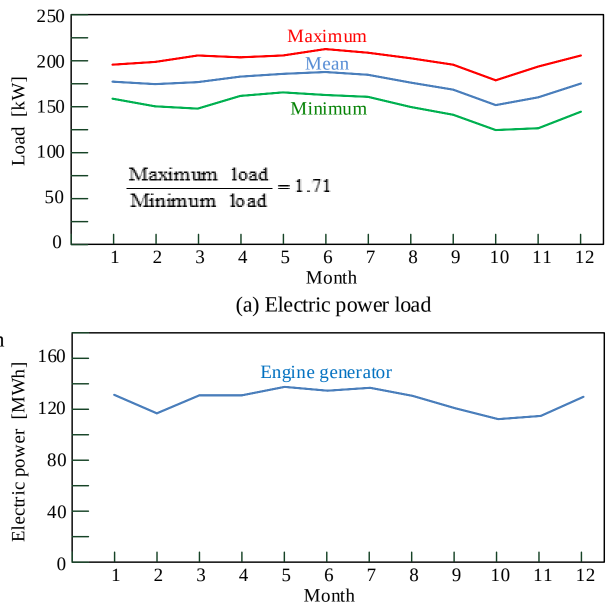

(a) Electric power load

(b) Monthly power supply

Fig. 8 Monthly electric power consumption of the 51st party

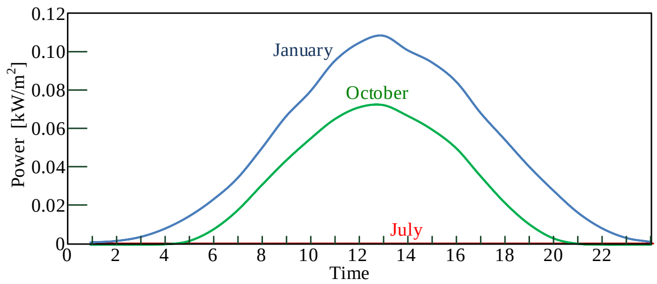

Fig. 6 Performance of photovoltaics

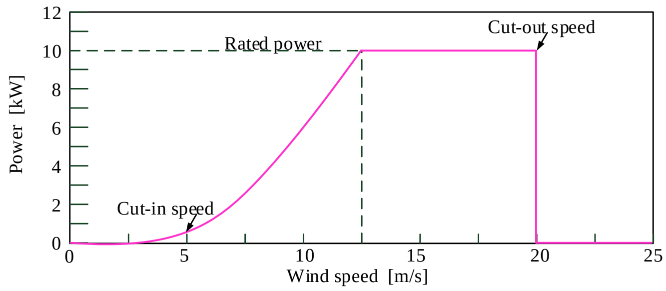

Fig. 7 Power performance of wind power generator

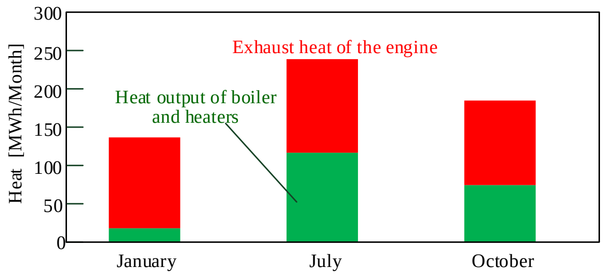

Fig. 9 Monthly heat demand of the 51st party

Figure 5 represents the concentration power system (240 kW) currently installed in the Syowa Base, the load factor of the distributed power supply system (113 kW, three sets) assumed in this study, and the efficiency characteristics of electricity and thermal power. Although the maximum efficiency of the 240 kW engine generator is higher than the 113 kW engine generator, the amount of exhaust heat from the 113 kW engine generators at the same load factor is more than that from the 240 kW generators, as seen in Fig. 5. Equation (4) is an approximate expression of the load factor of the engine generator and thermal power efficiency.

[DOI: 10.1299/jtst.2014jtst0013]

$$\eta_{egh,i} = 0.001 \cdot \lambda_{eg,i}^2 - 0.2867 \cdot \lambda_{eg,i} + 41.60 \tag{4}$$

4.2 Heat pump

As shown in Fig. 4, the heat medium heated by engine exhaust supplied to the demand side (Heat demand A) is subsequently transferred to the heat storage tank, and then returned to the engine. As the low temperature heat source of the heat pump is the heat storage tank, and the heat source is higher than outside temperatures, COP regularity is taken as 4.0. Moreover, efficiency of the drive motor of the heat pump $\eta_{mt,i}$ is set to 0.9. The thermal power of the heat pump $h_{w2,i,t}$ is expressed by Eq. (5) from the energy flow, as shown in Fig. 4. Moreover, COP of the heat pump is defined by Eq. (6).

$$h_{w2,i,t} = h_{4,i,t} + l_{mt,i,t} = h_{2,i,t} - h_{w1,i,t} - h_{loss,i,t} + l_{mt,i,t} / \eta_{mt,i} \tag{5}$$

$$h_{w2,i,t} \Big/ l_{mt,i,t} = COP \; (= 4.0) \tag{6}$$

4.3 Green Energy Equipment

Figure 6 shows the output characteristics of photovoltaics with a power generation efficiency of 18 %, which is calculated on the basis of the amount of global solar radiation in the summer (January), midterm (October), and winter (July) at the Antarctic Syowa Base. In addition, Fig. 7 shows the output performance characteristics of the wind power generation in the base. The cut-in and cut-out speeds of the wind power generator are 5 m/s and 20 m/s, respectively, and the rated power more than a wind-speed of 12.5 m/s is 10 kW in one set. Moreover, the electricity power e_{wp} of wind power generation in the wind-velocity range from cut-in velocity (5 m/s) to the rated speed (12.5 m/s) can be obtained from the approximate expression given by Eq. (7) and by Fig. 7.

$$e_{wp} = -0.000357 \cdot v_{wp}^4 + 0.0102 \cdot v_{wp}^3 - 0.00561 \cdot v_{wp}^2 - 0.1038 \cdot v_{wp} + 0.0612 \tag{7}$$

5. Setting of energy demand characteristics

5.1 Energy Demand Characteristics

Figure 8 (a) shows the measurement results of the average, minimum, and maximum values of the power load for every month in 2009–2010 for the 51st party, and Fig. 8 (b) presents the additional monthly production of electricity by the engine generator (National Institute of Polar Research Japan, 2011). The maximum power load for one year is 1.71 times the minimum load seen in Fig. 8 (a). The power load experiences a 20% fluctuation around the average value. Figure 9 is the amount of power for the engine exhaust heat of the summer, winter, and midterm months for the 51st party, and heat consumption and supply calculated from the fuel calorific value of the boiler and the heater for space heating. The percentages of the exhaust heat supplied from the engine generator are 86% and 51% for summer and winter demands, respectively.

5.2 Load setting

On the basis of the power load of the Syowa Base measured by Nishikawa et al. (National Institute of Polar Research Japan, 2011), the power and heat loads of the Syowa Base will increase in 2011 compared with that in 2010. Although it is expected that the power load is affected by outside temperature, fluctuations in the power load occur because of the inestimable load of observation equipments, such as household-appliances. In this study, the power load of a representative day refers to the actual values of power load, and determines the power load as the range of the minimum and maximum under the application of a random number. The power load $\Delta e_{load,month,t}$ in the time t of a representative day in a representative month is calculated from Eq. (8). Where, θ is a random number from 0 to 1. The 1st term on the right-hand side is an adjustment term of power load by the difference of a target room temperature (T_O) at the base, and the outside air temperature ($T_{\infty,t}$) in time t . Moreover, the 2nd term on the right-hand side represents the load change in the range of the maximum ($\Delta e_{load,month,\max}$) and minimum ($\Delta e_{load,month,\min}$) power load in a representative month. Figure 10 (a) is an example of the power load calculation results by Eq. (8).

[DOI: 10.1299/jtst.2014jtst0013]

$$\Delta e_{load,month,t} = \Delta e_{load,month,ave} \cdot \frac{24 \cdot \left(T_o - T_{\infty,t}\right)}{\sum_{t=1}^{24}\left(T_o - T_{\infty,t}\right)} + \left(\Delta e_{load,month,\max} - \Delta e_{load,month,\min}\right) \cdot \left(\theta - 0.5\right) \tag{8}$$

Equation (9) is the heat load of the whole SBMG in the sampling time t of a representative day and month. The 1st term on the right-hand side of Eq. (9) adjusts the magnitude of heat load based on the difference of target and outside temperatures, $\Delta h'_t$ is the actual past value of fuel consumption in the boiler and heater for space heating in the time t. The 2nd term on the right hand side is the actual amount of exhaust heat from past engine generator data. The measurement results (National Institute of Polar Research Japan, 2011) according to Nishikawa et al. for 2010–2011 and the actual results by the 51st party for 2009–2010 (Nishikawa, et al., 2011, National Institute of Polar Research Japan, 2011) are given for $\Delta h'_t$ and $h'_{eg,t}$. An example of heat load pattern calculated by Eq. (9) is shown in Fig. 10 (b).

$$\Delta h_{load,t} = \Delta h'_t \cdot \frac{\left(T_o - T_{\infty,t}\right)}{\sum_{t=1}^{24}\left(T_o - T_{\infty,t}\right)} + h'_{eg,t} \tag{9}$$

Where,

$$h'_{eg,t} = 1.5486 \cdot \lambda_{eg,t} + 45.7368 \tag{10}$$

$\lambda_{eg,t}$ is the load factor of the engine generator in the sampling time t, and Eq. (10) was obtained from the measurement results by Nishikawa et al. (National Institute of Polar Research Japan, 2011).

6. Analysis Methods

6.1 Definition of energy system

The energy system presently at the Syowa Base is defined as the conventional system. The power supply of this system consists of one set of 240 kW diesel generators, heat supplies by engine generator exhaust heat, electric heaters, kerosene boilers, an oilstove, and a solar collector. In system A, electricity is supplied from three sets of 113 kW diesel generators, and space heating is supplied by heat pumps using engine exhaust heat, heat storage tanks, backup boilers, and a kerosene boiler or an oilstove in some buildings. Furthermore, System B introduces electric storage heaters instead of kerosene boilers, and oilstoves are introduced into System A. However, to accommodate the large load of electric storage heaters used in System B, as described in Section 7.3, this study also examines the introduction of electric storage heaters into areas, such as a residence buildings, accompanied by heat pumps.

6.2 Climate conditions

Figure 11 shows the meteorological data (outside air temperature, wind velocity, and amount of insolation) at the Syowa Base (Nishikawa, et al., 2011, National Institute of Polar Research Japan, 2011, Homepage of Japan Metrological Agency, 2014). Figure 11 (a) presents the average outside air temperature for January (summer), July (winter), and October (midterm) at the Syowa Base for the 51st party. Although daytime air temperature in January and October was slightly higher than at night, there is almost no difference through the day in July due to lack of solar radiation. Figure 11 (b) shows the mean wind for every sample period of every month. Every month, the mean wind fluctuates greatly from 6:00 to 13:00. Figure 11 (c) depicts the average global solar radiation for each sample period on the representative day of every month. The most solar radiation at the Syowa Base occurs in the summer season. In winter, photovoltaics cannot be used because a lack of insolation.

6.3 Flow of operation analysis

The flow of operational analysis of the proposed SBMG (Fig. 2, System B) is shown in Fig. 12. (a)–(p). The first is inputting the meteorological data of the Syowa Base into the analyzing program (a), as shown in Fig. 11. In the next step,

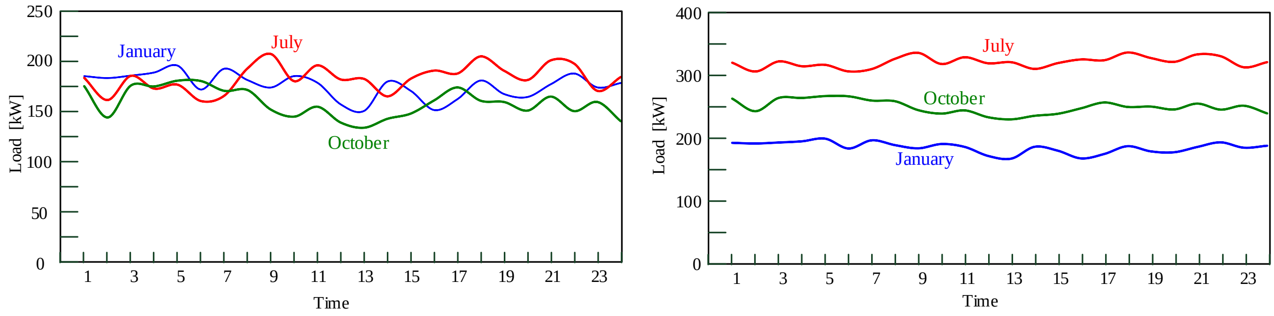

(a) Electric power demand (b) Heat demand

Fig. 10 Power demand models

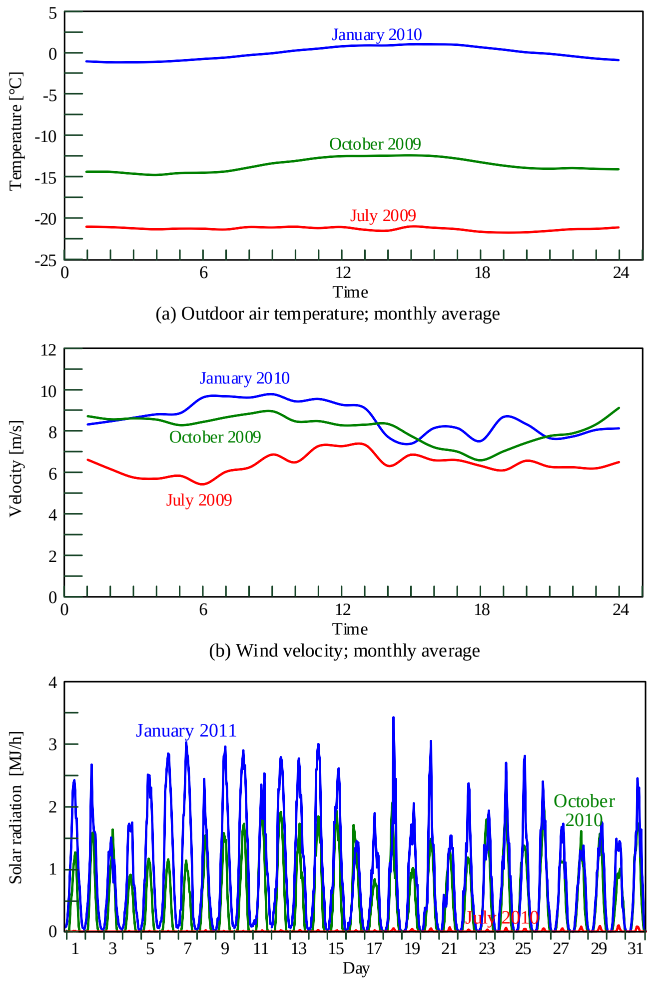

(a) Outdoor air temperature; monthly average

(b) Wind velocity; monthly average

(c) Global solar radiation

Fig. 11 Meteorological data at Syowa base

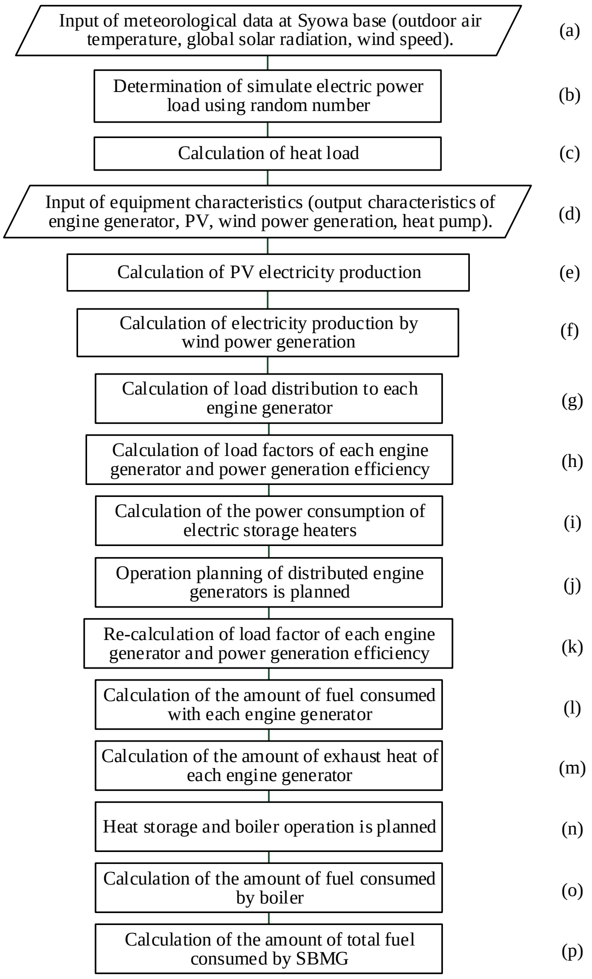

Fig. 12 Analysis flow

the pattern of the power load and heat load is calculated according to Section 5.2 ((b) and (c)), and the equipment characteristics of the power sources and heat pumps described in Section 4 are then added in (d). The power of the photovoltaics and wind power generation for each time period is used to calculate the equipment characteristics described above in Eq. (7), Fig. 6, and Fig. 7 ((e) and (f)). The load of each engine generator for each sample time is decided from the power load of the operation method described in Fig. 3 (g). The load factor of each engine generator is set up at 100%, 50%, or 0% and the power generation efficiency (Eq. (3)) of each engine generator is calculated (h). In the next processing step (i), the operating pattern of each engine generator, accumulation of electricity, and electric discharge are planned on the basis of the system operation method described in Fig. 3 (c). The load factor and power generation efficiency are then recalculated for the operating pattern of each engine generator for each sample time described above (j). From the power-generation efficiency of each engine generator, fuel consumption and the amount of exhaust heat for each time period of the representative day can be calculated by referring to Fig. 13 ((k), (l)). From the power output pattern of the exhaust

[DOI: 10.1299/jtst.2014jtst0013]

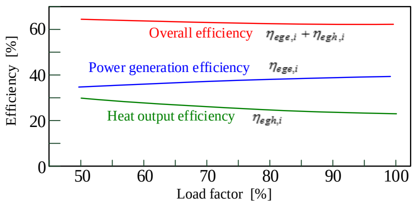

Fig. 13 Efficiency characteristics of the 113 kW engine generator installed in SBMG

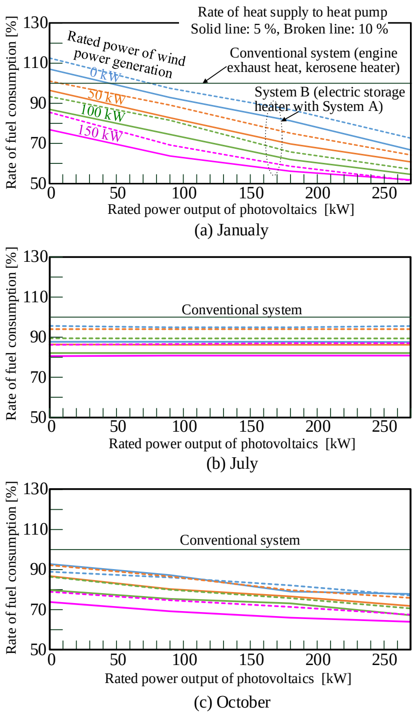

Fig. 14 Analysis results of fuel consumption rate of System B relative to the conventional system. Heat supply to all buildings except the power-generation (A_0), residence (A_1, A_2), warehouse and sewage disposal (A_3), administration (A_4) buildings, which are shown in Fig. 1.

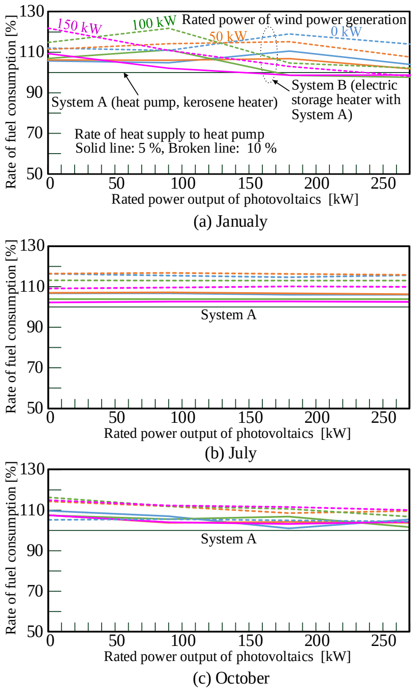

Fig. 15 Analysis results of fuel consumption rate of System B relative to System A. Heat supply to all buildings except the power-generation (A_0), residence (A_1, A_2), warehouse and sewage disposal (A_3), administration (A_4) buildings, which are shown in Fig. 1.

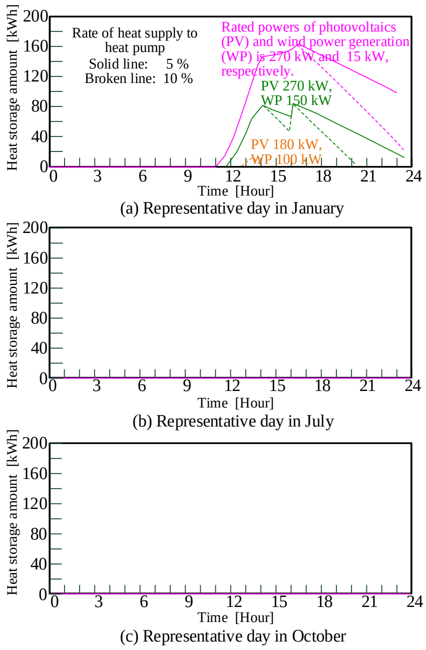

Fig. 16 Analysis results of the operation of electric storage heaters in System B

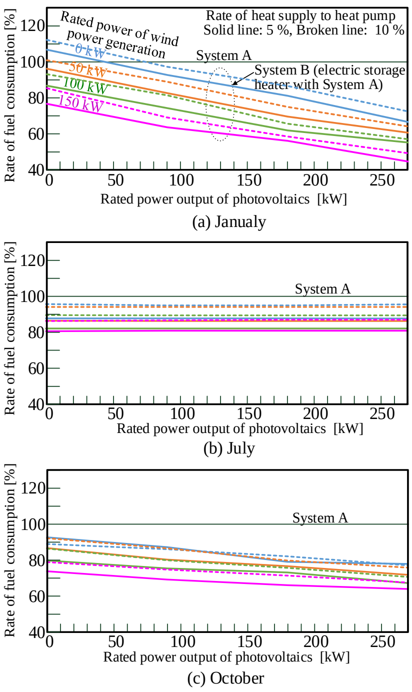

Fig. 17 Analysis results of fuel consumption rate of System B relative to the conventional system. Heat supply to the following buildings: power-generation (A_0), residence (A_1, A_2), warehouse and sewage disposal (A_3), and administration (A_4) buildings, which are shown in Fig. 1.

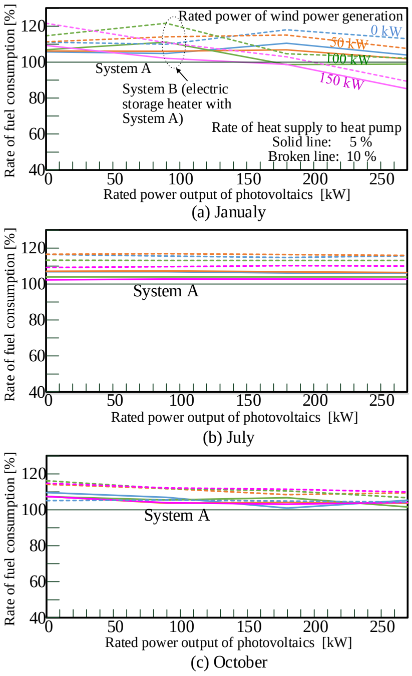

Fig. 18 Analysis results of fuel consumption rate o System B to the System A. Heat supply to thi following buildings: power-generation (A_0) residence (A_1, A_2), warehouse and sewag disposal (A_3), and administration (A_4) buildings which are shown in Fig. 1.

heat for each engine generator (Eq. (4)), operation of heat output of heat pumps (Eq. (5)), heat storage, or heat output within heat storage tanks and backup boilers is planned (m). As a result, fuel consumption in each boiler is calculable (n). Fuel consumption in a representation day is obtained by adding fuel consumption of each engine generator and all backup boilers (o).

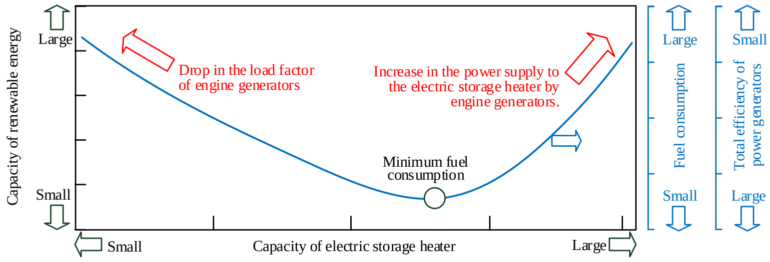

Fig. 19 Capacity optimization of the electric storage heater

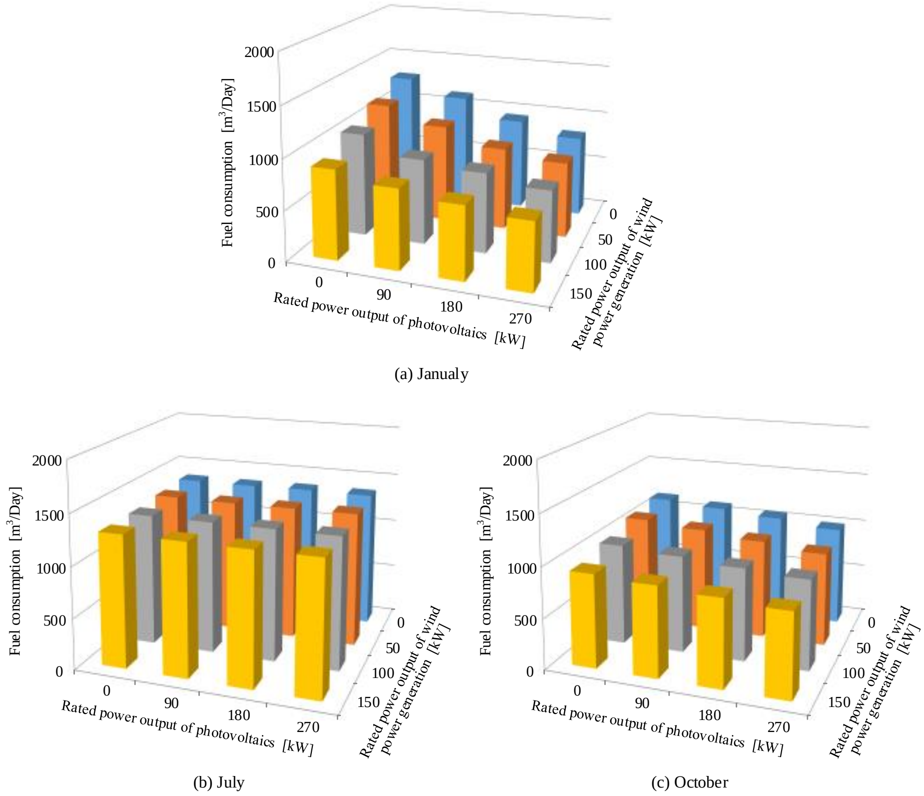

Fig. 20 Analysis results of the proposed system (System B). 5 % of heat supply to the heat pump.

7. Analysis results

7.1 Introductory Effect of Electric Storage Heaters

Figures 14 and 15 show the analysis results of the relationship between the rate of renewable energy output (photovoltaics and wind power generation) and fuel consumption, when System B with electric storage heaters is introduced into the Syowa Base. Electric storage heaters were introduced in the 70 buildings of the Antarctic Syowa Base, with the exception of power-generation (A_0), residence (A_1, A_2), storage and sewage disposal (A_3), and administration (A_4) buildings. Exhaust heat from an engine generator (conventional system) or a heat pump using engine exhaust heat (System A) is used to heat the buildings described above. Figure 14 shows the rate of fuel consumption over the conventional Syowa Base energy system, and Fig. 15 presents the analysis of the rate of fuel consumption over System A. The storage capacity of electric storage heaters is set using the output quantity of the heat pump as a reference. The heat storage capacity of electric storage heaters was set to 5% or 10% of the heat pump output on a representative day in this analysis. The ratios of heat supply from heat pumps and electric storage heaters that are shown in Figs. 14 and 15 were 95:5 (solid line) and 90:10 (broken line).

The result from every representative day for all months (Fig. 14), indicate that the introduction of electric storage heaters can contribute to a reduction in fuel consumption compared with the conventional system. When renewable energy is supplied to electric storage heaters, fossil fuel use will be reduced by a great extent as the output of photovoltaics and wind power generation is increased. However, because solar radiation in July (winter) is very slight, the output of photovoltaics does not influence fuel consumption of the base, as shown in Fig. 14 (b). Figure 15 shows a comparison

[DOI: 10.1299/jtst.2014jtst0013]

with System A, where electric storage heaters are installed in all but the large building group of heat loads, such as a residence building; despite this, the fuel reduction effect by electric storage heaters is dramatically restrictive. The electric storage heater becomes advantageous when power from renewable energy is high, such as in January (140 kW or more of photovoltaics, 150 kW or more of wind power generation), as shown in Fig. 15 (a).

7.2 Heat storage characteristics of electric storage heaters

To reduce fuel consumption of the base through the introduction of electric storage heaters, a sufficient quantity of renewable energy is required. As Fig. 11 shows using meteorological data, the wind velocity and amount of insolation in July (winter) are smaller than in the summer, with a substantial decrease in insolation in October (midterm) relative to the summer season. Therefore, the optimal equipment capacity for each season differs greatly. As a result, thermal storage by electric storage heaters was not operated other than in January (Fig. 16 (a)). Therefore, to utilize electric storage heaters for winter with greater heat demand, a substantial increase in the capacity of wind power generation is needed. On the other hand, even if the rated capacity of photovoltaics increases, the hours of operation of electric storage heaters year round do not. By introducing much more wind based renewable energy into the Syowa Base, electric storage heaters are effectively utilizable throughout the entire year. However, with an excess of renewable energy, the limited heat storage amount of electric storage heaters make it superfluous as suggested from the analysis results of Fig. 16 (a). Accordingly, even if renewable energy increases across all time periods or seasons with little heat demand, the fuel reduction effect of electric storage heaters is small.

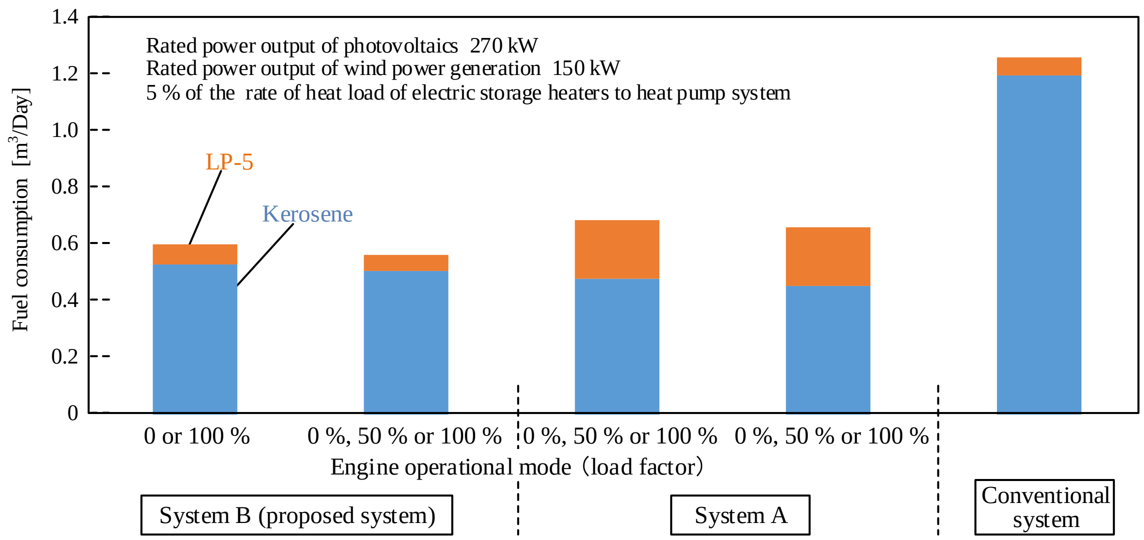

Fig. 21 Analysis results of fuel consumption in January

7.3 Introductory increase in electric storage heaters and fuel reduction effect

Electric storage heaters are purposefully introduced into some building groups with large space heating demands (power-generation, residence, storage and sewage disposal, and administration buildings) to raise the operating ratio of electric storage heaters. Figures 17 and 18 show the relationship between the rated output of renewable energy and fuel consumption when System B, which was accompanied by electric storage heaters, was introduced into the base. Heat pumps using engine exhaust heat, backup boiler, and heat storage tank, as shown in Fig. 1 (b), were introduce into the house group with large space heating demands. Electric storage heaters account for the insufficiency of heat supplied by heat pumps and reduce the fuel for the backup boilers, as shown in Fig. 1 (b). Figure 17 indicates the rate of fuel consumption over the conventional Syowa Base energy system, while Fig. 18 shows the rate of fuel consumption over System A. Areas where the results of Figs. 17 and 18 differ from that of Figs. 14 and 15 are the renewable energy conditions in January (more than the 250 kW rated-output of photovoltaics and the 150 kW rated-output of wind power generation). For the conditions described above, fuel consumption of the base was reduced by the introduction of electric storage heaters.

[DOI: 10.1299/jtst.2014jtst0013]

7.4 Introduction of electric storage heater, and fuel consumption of the Syowa Base

Figure 19 shows the relationship between the capacity (rated output) of electric storage heaters and renewable energy, an operating time of electric storage heaters using power of engine generators, load factors of the engine generators, the power generation efficiency of engine generators, and fuel consumption of the base following the introduction of electric storage heaters into the Syowa Base. The reduction of fuel consumption in the Syowa Base through the introduction of electric storage heaters requires suitable ranges of the conditions described above. Furthermore, for the minimization of fuel consumption, the rated capacity of engine generators, photovoltaics, wind power generation, and electric storage heaters needs to be appropriately selected.

7.5 Fuel consumption characteristics of the Syowa Base

Figure 20 shows the analysis results of fuel consumption in a representative day of every month. These figures represent the results of the proposed system (System B) after changing the cell area of photovoltaics and installed number of wind power generators in January (summer), July (winter), and October (midterm). Most fuel consumption occurs on the base in July when the power of photovoltaics is the lowest of all the months. However, if photovoltaics with a larger area and more wind power generators are introduced at the Syowa Base in January or October, fuel consumption will reduced. For SBMG, a large difference in fuel consumption during summer and winter exists because of the variation in photovoltaic electricity production.

Figure 21 shows the energy consumed on a representative January day at the Antarctic Syowa Base with SBMG. The engine operational mode of the horizontal axis sets the load factors of the engine generator, as described in Fig. 3; accordingly, the operating mode is set at 0% (neutral operation), 50%, or 100% of load factor, or the mode is set at 0% or 100%. The reduction of fuel consumption by setting the load factor to 0%, 50%, or 100% of the engine generators is larger than setting of the load factors of 0% or 100%, as shown in Fig. 21. System B can reduce fuel consumption of the Syowa Base by 15% in January compared with System A. Moreover, fuel consumption in January with System B is half that of the conventional system. However, most fuel consumption savings by System B are not obtained in July and October. The introductory wind power generation capacity is capable of being increased; the output of wind power generation varies minimally with season, as described above. Furthermore, power supply and heat radiation to electric storage heaters must be made constant, as shown Fig. 3 (c), to optimize the operation under the objective of minimizing fuel consumption.

7.6 Cost analysis

Below, the results of the cost analysis of the proposed system is described.

7.6.1 Equipment cost

The principal equipment, such as an engine generator, a heat pump, an electric storage heater, and a heat storage tank, assumes the common products currently used in Japan. Therefore, it is expected that such equipment costs are the same as a common popular product. However, wind power generation and photovoltaics require the cost for weather out a strong blizzard. The reinforcement cost described in the top is due to be estimated from results of local experiment.

7.6.2 Running cost

Although maintenance of operation of the conventional large-sized power generator had taken the personnel expenses, the running cost of the proposed system is only a fuel cost of the engine generator. Proposed compact engine power generators are replaced with equipment conveyed from Japan.

8. Conclusions

Reduction of the fuel transportation from Japan and the environmental impact of the exhaust gas are the small-scale energy network problems of the present Antarctic Syowa Base (SBMG) with a 240 kW diesel engine generator as the main power supply. Therefore, the Syowa Base is considering extensive introduction of photovoltaics and wind power generation to drastically increase the local supply and consumption of energy. The method of distributing small-capacity engine generators and the operation of heat pumps accompanied by high COP using engine exhaust heat were investigated in this study. The periods with surplus power increase with the amount of renewable energy to SBMG. Therefore, this study considered thermal storage of renewable energy by installing electric storage heaters, which are currently widely

[DOI: 10.1299/jtst.2014jtst0013]

used by super airtight and super insulation houses of the cold district, in each building of SBMG. When the hybrid heat supply system of heat pump systems using engine exhaust heat and electric storage heaters was introduced in SBMG, the following conclusions were made about the reduction effect of the introductory rate of renewable energy and fuel consumption of the base.

(1) When electric storage heaters are introduced into buildings, including residence buildings with higher heat demand, the fossil fuel of the base will be reduced by the heat storage of renewable energy. However, in order to obtain this effect year round, extensive introduction of wind power generation is more effective than the photovoltaics because of seasonal stability in output. Moreover, when the amount of renewable energy is increased substantially, it is the assumption of this study that the fuel reduction is large.

(2) System B (type of heat pumps and electric storage heaters hybrid system) can reduce fuel consumption of the Syowa Base in January by 15% relative to System A (type of the heat pump system used in previous studies), and reduces fuel consumption to half that of the conventional system. However, fuel consumption by System B in July and October, periods of high heat demand, was not different from that of System A. A way to further reduce fuel consumption of the base is by introducing a large amount of wind power generation with little seasonal output variability. Moreover, to minimize fuel consumption of the base further it is necessary to optimize the amount of heat storage and heat radiation of electric storage heaters.

9. Nomenclature

e	:	Electric power [kW]	θ	:	Random number between 0 and 1
e_{pst}	:	Power load of Syowa base [kW]	Subscript		
Δe	:	Consumption of electric power [kW]	ave	:	Average
h	:	Heat [kW]	bo	:	Boiler
h'_{eg}	:	Record of past of engine exhaust heat [kW]	bt	:	Battery
Δh	:	Consumption of heat [kW]	eg	:	Engine
$\Delta h'$	:	Fuel consumption of boiler and heater for space heating [kW]	esh	:	Electric heat storage heater
l	:	External work [kW]	gt	:	Generator
N	:	The number	hp	:	Heat pump
T_o	:	Target temperature [K]	hst	:	Heat storage tank
T_∞	:	Outside temperature [K]	$load$	:	Load
t	:	Sampling time [h]	$loadh$	:	Thermal load
Greek characters			$loss$	:	Loss
η	:	Efficiency	mt	:	Electric motor of heat pump
η_{ege}	:	Power generation efficiency	pst	:	Electric power load
η_{egh}	:	Heat output efficiency	pv	:	Photovoltaics
λ	:	Load factor [%]	pvu	:	Unit of photovoltaics
v	:	Wind speed [m/s]	wp	:	Wind power generator

References

Arteconi, A., Hewitt, N. J, and Polonara F., State of the art of thermal storage for demand-side management, Applied Energy, Vol.93, (2012), pp.371–389.

Chesi, A., Ferrara, G., Ferrari, L., Magnani, S. and Tarani, F., Influence of the heat storage size on the plant performance in a Smart User case study, Applied Energy, Vol.112, (2013), pp.1454–1465.

[DOI: 10.1299/jtst.2014jtst0013]

Dawei, W,, Hongdong, Y., Adam, H. and Anthony, P. R., Micro distributed energy system driven with preheated Croton megalocarpus oil–A performance and particulate emission study, Applied Energy, Vol.112, (2013), pp.1383–1392.

Homepage of Japan Metrological Agency. Retrieved from http://www.data.jma.go.jp/obd/stats/etrn/index.php?prec_no=99&block_no=89532&year=&month=&day=&view=, (2014).

Homepage of Telegraph Media Group Limited, Jeff Howell: what are the most efficient storage heaters?, Retrieved from http://www.telegraph.co.uk/property/propertyadvice/10182045/Jeff-Howell-what-are-the-most-efficient-storage-heaters.html, (2014).

Massimiliano, M., Paola, C. and Gaia, C., Paradigm shift in urban energy systems through distributed generation: Methods and models, Applied Energy, Vol.88, (2011), pp.1032–1048.

National Institute of Polar Research Japan. Present condition of the energy equipment of Syowa base, The 1st South Pole green energy use examination WG, (2011), pp.4–30.

National Institute of Polar Research Japan. Present condition of the energy equipment of Syowa base, The 2nd South Pole green energy use examination WG, (2011), pp.1–66.

Nishikawa, S., Abiko, H., Kurihara, J., Ishizawa, K. and Endo, N., Fundamental study for introduction of renewable energy into Syowa base, IEEJ transactions on power and energy, Trans. of IEE J, Vol.131, No.9, (2011), pp.778–785 (in Japanese).

Obara, S., Kawae, O., Kawai, M. and Morizane, Y., A study of small-scale energy networks of the Japanese Syowa base in Antarctica by distributed engine generators, Applied Energy, Vol.111, (2013), pp.113–128.

Tian, Y. and Zhao, C. Y., A review of solar collectors and thermal energy storage in solar thermal applications, Applied Energy, Vol. 104, (2013), pp.538–553.

Uisung, L., Elango, B. and Chung, J. N., An experimental evaluation of an integrated biomass gasification and power generation system for distributed power applications, Applied Energy, Vol.101, (2013), pp.699–708.

[DOI: 10.1299/jtst.2014jtst0013]